analytical chemistry

Article

pubs.acs.org/ac

Hairpin DNA-Assisted Silicon/Silver-Based Surface-Enhanced Raman Scattering Sensing Platform for Ultrahighly Sensitive and Specific Discrimination of Deafness Mutations in a Real System

Hui Wang,[†,§] Xiangxu Jiang,[†,§] Xing Wang,[‡,§] Xinpan Wei,[†] Ying Zhu,[†] Bin Sun,[†] Yuanyuan Su,[†] Sudan He,*[,‡] and Yao He*[,†]

[†]Institute of Functional Nano and Soft Materials and Collaborative Innovation Center of Suzhou Nano Science and Technology, Jiangsu Key Laboratory for Carbon-Based Functional Materials and Devices, and [‡]Cyrus Tang Hematology Center, Jiangsu Institute of Hematology, First Affiliated Hospital, and Collaborative Innovation Center of Hematology, Soochow University, Suzhou 215123, China

Supporting Information

ABSTRACT: Surface-enhanced Raman scattering (SERS) is well-recognized as a powerful analytical tool for ultrahighly sensitive detection of analytes. In this article, we present a kind of silicon-based SERS sensing platform made of a hairpin DNA-modified silver nanoparticles decorated silicon wafer (AgNPs@Si). In particular, the AgNPs@Si with a high enhancement factor (EF) value of ~4.5×10^7 is first achieved under optimum reaction conditions (i.e., pH = 12, reaction time = 20 min) based on systematic investigation. Such resultant AgNPs@Si is then employed for construction of a silicon-based SERS sensing platform through surface modification of hairpin DNA, which is superbly suitable for highly reproducible, multiplexed, and ultrasensitive DNA detection. A detection limit of 1 fM is readily achieved in a very reproducible manner along with high specificity. Most significantly, for the first time, we demonstrate that the silicon-based SERS platform is highly efficacious for discriminating deafness-causing mutations in a real system at the femtomolar level (500 fM), which is about 3−4 orders of magnitude lower than that (~5 nM) ever reported by conventional detection methods. Our results raise the exciting potential of practical SERS applications in biology and biomedicine.

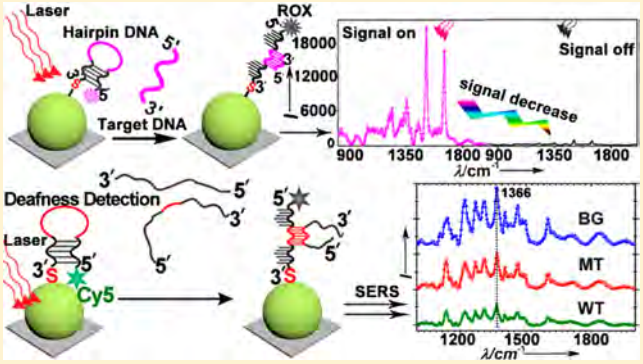

Surface-enhanced Raman scattering (SERS), known as a highly attractive phenomenon, has been employed for wide-ranging physical, chemical, and biological studies. Typically, SERS enables remarkable amplification of normal Raman signals, which are ideally amplified by factors up to 10^{12-14}, affording the possibility to acquire the characteristic fingerprint of low-concentration analytes. In addition, SERS features narrow Raman bands, offering opportunities for multiplexed assays with minimal background interference.[1−6] Consequently, taking advantages of these unique merits, much effort has been devoted to the fabrication of a myriad of ingenious SERS biosensors to identify and detect an array of biological and chemical analytes, such as small bioactive molecules,[4,7] trinitrotoluene (TNT),[8] DNA,[1,9,10] proteins,[11,12] and heavy metallic ions,[13,14] etc.

It is worth pointing out that most of reported strategies for DNA detection are generally based on "signal-on" procedure, in which DNA hybridization leads to distinct enhancement of SERS signals. For example, Braun et al. introduced a class of Ag nanoparticles (AgNPs)-based SERS probes for unambiguous identification of single-stranded DNA.[15] Typically, a significant SERS signal could be observed by DNA hybridization-assisted assembly process, forming the Ag film/DNA/AgNPs sandwich structures. Kang et al. developed a kind of particle-on-wire sensor made of DNA-modified Au particles, whose SERS intensities were gradually enhanced along with increasing of DNA concentrations, allowing a low DNA detection limit of 10 pM.[10] Cao et al. employed Ag-stained gold particles to construct a kind of sandwiched assay to produce enhanced SERS signals in DNA microarray format.[2] More recently, our group reported a kind of capture/target/reporter DNA-modified silicon nanowires (SiNWs)-based sandwiched biosensor. In that case, distance between organic dyes and SERS substrates became close, which was due to hybridization between targeted DNA and reported DNA. As a result, SERS intensities were distinctly amplified and low-concentration (e.g., ~10 fM) DNA was readily detected.[16] On the other hand, hairpin featuring a stem−loop structure has been recently used for fabricating high-quality biosensors with higher sensitivity

Received: February 1, 2014
Accepted: July 7, 2014
Published: July 7, 2014

   dx.doi.org/10.1021/ac501675d | *Anal. Chem.* 2014, 86, 7368−7376

and lower background signals.[17,18] Specifically, Fan et al. employed electroactive reporter (e.g., ferrocene carboxylic acid) tagged gold electrodes for constructing electrochemical DNA sensors.[19] Hybridization with target DNA resulted in alteration of distance between the labels and electrode surface, yielding distinct change of electrochemical signals and allowing sensitive discrimination of low-concentration (10 pM) 17-mer target DNA. Du et al. immobilized tetramethylrhodamine-labeled hairpin DNA on a gold substrate to construct high-quality fluorescent biosensors with a detection limit of 10 nM.[20] Recently, taking advantages of unique merits of silicon nanomaterials (e.g., unique optical/electronic/mechanical traits, large surface-to-volume ratios, and facile surface functionality, etc.), our group has successfully developed a silicon-based platform for various biosensing applications.[21−28] In particular, we employed AuNPs-coated SiNWs as novel fluorescent quenchers with high quenching efficiency and robust salt stability for construction of hairpin DNA-assisted silicon-based molecular beacons (MBs), which was suitable for detection of low-concentration DNA (∼50 pM).[21] While these exciting progresses suggest hairpin DNA as an efficacious medium for design of high-performance sensors, few reports on SERS "signal-off" sensing strategies have been reported thus far.[29−31] Very recently, by utilizing AuNPs-decorated SiNWs whose surfaces were immobilized with stem−loop DNA probes, our group further developed a class of SiNWs-based "signal-off" SERS biosensor using hairpin DNA as capture probes and AuNPs as SERS substrates, allowing sensitive, reproducible, and multiplexed detection of DNA with low concentrations (e.g., 10 fM).[22] However, it is worth pointing out that this kind of SERS substrate is made of SiNWs, which requires relatively complicated synthetic procedures and post-treatment (e.g., oxide-assisted, metal-catalyzed vapor−liquid−solid and HF-assisted etching growth, etc.), severely limiting their practical applications.[32] In addition, as is well-known, AuNPs employed in the SiNWs-based SERS substrates generally exhibit much lower SERS enhancement effect than AgNPs, which is adverse to sensitivity of the SERS sensors.[33,34] Consequently, a continual and urgent search is still required to facilely construct hairpin DNA-assisted SERS sensors of high sensitivity and specificity for practical applications.

In the present study, to alleviate the above-mentioned problems, we herein introduce a kind of silicon-based SERS sensing platform made of hairpin DNA-modified AgNPs-decorated silicon wafer (AgNPs@Si). In particular, AgNPs are facilely in situ grown on silicon wafer via a facile and rapid (∼20 min) one-step reaction, producing the AgNPs@Si with an enhancement factor (EF) value of ∼4.5×10^7 under optimum reaction conditions (i.e., pH = 12, reaction time = 20 min). Such resultant AgNPs@Si is then employed for construction of silicon-based SERS sensing platform through surface modification of hairpin DNA, which is superbly suitable for reproducible, multiplexed, and ultrasensitive DNA detection. In particular, a detection limit of 1 fM is readily obtained in a very reproducible manner along with excellent specificity. Most significantly, for the first time, we further show that the silicon-based SERS platform is highly efficient for discriminating deafness-causing mutations in a real system at the femtomolar level (∼500 fM), which is 3−4 orders of magnitude lower than that ever reported by conventional methods [e.g., allele specific polymerase chain reaction (PCR),[35] DNA sequencing,[36] PCR-restriction fragment length polymorphism (PCR-RFLP) analysis,[36,37] etc.].

EXPERIMENTAL METHODS

Products and Devices. Phosphate-doped (p-type) silicon wafers (100, 0.01−0.02 Ω sensitivity) were bought from Hefei Kejing Materials Technology Co., Ltd. (China). Hydrofluoric acid (HF, ≥ 40%), hydrogen peroxide (H_2O_2, ≥ 30%), sulfuric acid (H_2SO_4, 98%), acetone, silver nitrate ($AgNO_3$, ≥ 99.8%), sodium hydroxide (NaOH, 98%), and 6-mercapto-1-hexanol (MCH) were bought from Sinopharm Chemical Reagent Co., Ltd. (Shanghai, China). DNA oligonucleotides were purchased from TAKARA Biotechnology (Dalian, China). All materials were used without further purification. Milli-Q water (Millipore) was used as solvent for preparation of all solutions. A microscope (FEI Quanta 200F) equipped with an energy-dispersive X-ray (EDX) spectroscopy facility and MultiMode V atomic force microscopy (AFM, Vecco Corporation, U.S.A.) were used for scanning electron microscopy (SEM) and AFM characterizations, respectively. An HR800 Raman microscope instrument equipped with a 633 nm He−Ne 20 mW laser (polarized 500:1) was employed for characterization of Raman spectra. For all measurements, the dominant parameters are as follows: $\lambda_{excitation}$ 633 nm, filter D2, objective 100× , NA 0.9, hole 1000 μm, slit 100 μm, grating 600 g mm^{-1}, and acquisition time 1 s.

Synthesis of the AgNPs@Si. The AgNPs@Si is produced through an established HF-etching method described in previous reports,[16,32,38] in which Ag^+ can be readily reduced by surface-covered Si−H bonds of silicon wafer, resulting in in situ growth of AgNPs with the same chemical state. In detail, the planar Si wafer was first cleaned by sequential ultrasonication in acetone and Milli-Q water for 10 min in each, then immersed into H_2SO_4 and H_2O_2 (v/v 3:1) for 30 min to remove organics and derive a thin oxide layer. The cleaned silicon wafer was further rinsed in 5% aqueous HF solution and kept for 30 min to produce H-terminated surface. Meanwhile, pH values of $AgNO_3$ aqueous solution (2.5 mM) were adjusted by adding HF (1.5%) or NaOH (0.1 M). Afterward, the as-treated silicon wafer was immediately submerged into silver nitrate aqueous solution (2.5 mM) with different pH values (e.g., 1, 5, 8, 10, 12, 13, and 14) for 20 min, producing seven kinds of AgNPs@Si at different pH values. On the basis of established protocol reported elsewhere,[39] the as-prepared AgNPs@Si was washed using Milli-Q water and then dried under N_2 gas and collected as SERS-active substrates for the latter experiments.

SERS Mapping. The prepared AgNPs@Si was rinsed in the solution of 1×10^{-8} M rhodamine 6G (R6G) for 20 min and then dried under N_2 gas for SERS detection.

Enhancement Factor Calculation. The enhancement factors (EF) of AgNPs@Si are estimated through the following equation reported elsewhere as follows:[39−43]

$$EF = (I_{SERS}N_{bulk})/(I_{bulk}N_{SERS}) \quad (1)$$

where I_{SERS} and I_{bulk} are the peak intensities of the SERS and Raman (non-SERS), respectively. N_{SERS} represents the molecular number of organic dyes on the AgNPs@Si substrate, and N_{bulk} is the molecular number of organic dyes absorbed in a bulk sample. Herein for SERS detection, a volume V_{SERS} of R6G aqueous solution is immersed to an area of S_{SERS} at a concentration of C_{SERS} on the AgNPs@Si substrate. For normal Raman spectra, a volume V_{bulk} of R6G is immersed to an area of S_{bulk} at a concentration of C_{bulk} on the pure silicon substrate. The foregoing equation thus becomes

dx.doi.org/10.1021/ac501675d | Anal. Chem. 2014, 86, 7368−7376

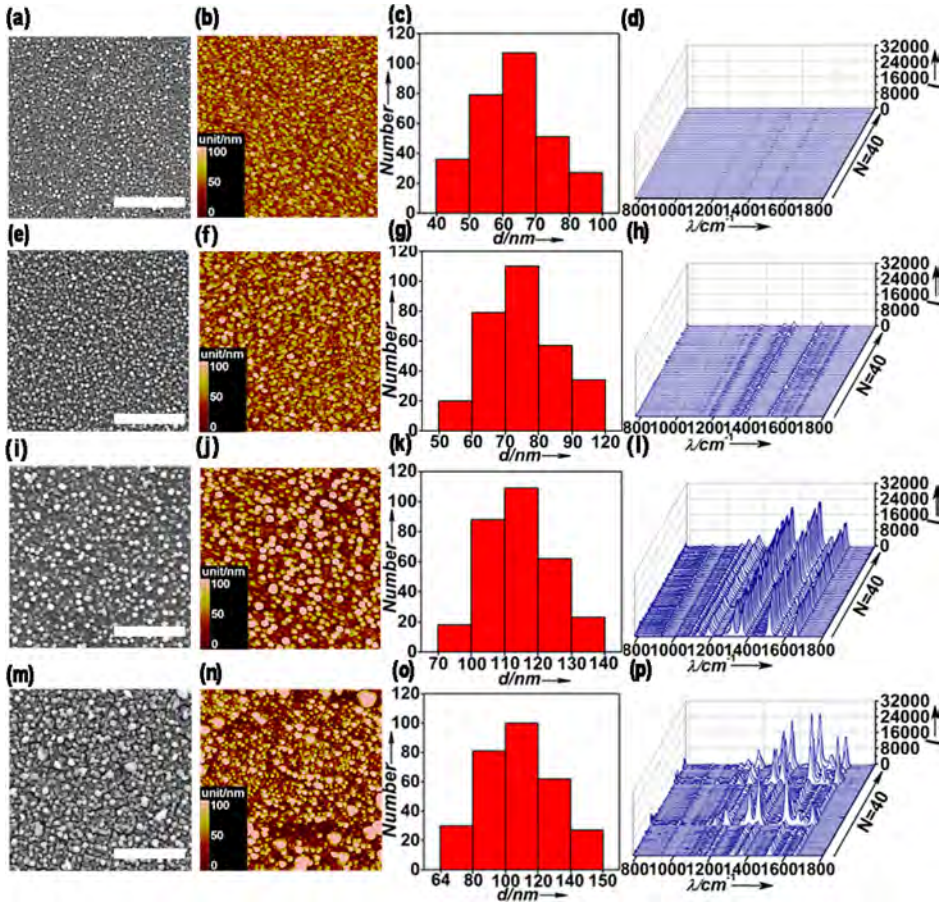

Figure 1. Typical SEM and AFM topographic images of the AgNPs@Si with different AgNPs size distributions and corresponding individual mapping spectrum of R6G submerged on the surface of AgNPs@Si recorded from 40 random dots at varying pH values (a–d, pH = 1; e–h, pH = 5; i–l, pH = 12; m–p, pH = 14), respectively. The scale bars in SEM images indicate 5 μm. The AFM images are collected from an area of 5.0 × 5.0 μm^2.

$$EF = (I_{SERS}/I_{bulk})(S_{SERS}V_{bulk}C_{bulk})/(S_{bulk}V_{SERS}C_{SERS}) \quad (2)$$

In our experiment, 12 μL of 10^{-9} M R6G aqueous solution was dispersed to the AgNPs@Si substrate at pH in the range of 1–14, while 12 μL of 10^{-2} M R6G was dispersed to the pure silicon wafer. The peak intensities located at 1364 cm^{-1} ascribed to the C–C stretching mode are 2 × 10^5 for the AgNPs@Si substrate and 2500 for the silicon wafer.[39,44,45] Assuming that all the organic molecules distributed in the area irradiated by the laser are illustrated and contribute to the Raman and SERS spectra, based on eq 2, the average EFs were calculated to be 3.6 × 10^5, 2.8 × 10^6, 5.1 × 10^6, 2.3 × 10^7, 4.5 × 10^7, 1.4 × 10^7, and 1.1 × 10^7 for the AgNPs@Si prepared at pH values of 1, 5, 8, 10, 12, 13, and 14.

DNA Detection by Using the Silicon-Based SERS Sensor. The DNA self-assembly procedure has been well-described in previously reported protocol.[21,22] Briefly, the prepared AgNPs@Si substrate was originally incubated with 50 μL of immobilization buffer containing 1 μM DNA (10 mM phosphate, pH 7.0, Supporting Information Table S1) for 24 h at room temperature. 1 M NaCl phosphate-buffered solution was added to the mixture to yield a final concentration of 0.1 M for 14 h to ensure sufficient self-assembly between thiolated-DNA and AgNPs@Si. Afterward, the hairpin DNA-modified AgNPs@Si was fully purified by washing three times with 0.1 M phosphate-buffered saline (PBS) buffer and further dried with N_2 gas, followed by hybridization with target DNA of serial concentrations (0.001–100 pM) in hybridization buffer (10 mM Tris–HCl, 100 mM KCl, and 1 mM $MgCl_2$, pH 8.0) for 2.5 h at 37 °C. The resultant sample was subsequently washed using PBS solution to fully remove excess DNA and finally dried with N_2 gas for following SERS detections. Identical manipulations were repeated for detection of the single-based-mismatched DNA. On the basis of SEM and AFM images, 1.5 × 10^7 AgNPs of 100 nm were immobilized on the specific silicon wafer. Taken together with our previous calculated results, i.e., 44 hairpin DNA probes were assembled on ~15 nm AgNPs,[46,47] we thus estimated that 2.9 × 10^{10} probes were assembled on the prepared AgNPs@Si substrates. It is worth noting that the SERS intensities were gradually enhanced accompanied by assembly of more stem–loop DNA with the AgNPs@Si and eventually reached a threshold when DNA sites were saturated.[48]

For multiplexed DNA assay, three kinds of hairpin DNA (1 μM, Supporting Information Table S2) tagged with ROX (6-carboxy-X-rhodamine), FAM, or Cy5 were first mixed in 50 μL of assembly buffer (10 mM phosphate, pH 7.0) at room temperature. Thereafter, the AgNPs@Si was immersed in the resultant mixture solution for 24 h in a sealed centrifuge tube, followed by 14 h of treatment with 0.1 M NaCl phosphate-buffered solution, producing the hairpin DNA-modified AgNPs@Si. Afterward, three types of target DNA (1 pM) were separately hybridized with the prepared hairpin DNA-modified AgNPs@Si in hybridization buffer (10 mM Tris–

dx.doi.org/10.1021/ac501675d | Anal. Chem. 2014, 86, 7368–7376

HCl, 100 mM KCl, and 1 mM $MgCl_2$, pH 8.0) at 37 °C for 2.5 h. The resultant sample was simultaneously washed using Milli-Q water and then dried with N_2 gas, which was ready for detection of multiplexed DNA.

Preparation of PCR Products. In the PCR reaction, the wild-type or mutant *SMAC/DIABLO* plasmid DNA described previously was used as the specific template for amplifying the full length wild-type or mutant form of *SMAC/DIABLO* DNA.[49] These PCR products were further extracted by using NucleoSpin gel and PCR clean-up kit (MACHEREY-NAGEL). The following primers were used in this experiment: primer-F, ATGGCGGCTCTGAAGAGTTGGCTG; primer-R, TCA-ATCCTCACGCAGGTAGGCCTC.

The PCR reaction mixture was prepared using 100 ng of template DNA, 0.5 μL of Phusion DNA polymerase containing 10 μL of 5 × Phusion HF buffer, 4 μL of 2.5 mM dNTP, and 2.5 μL each of 10 μM forward and reverse primers, 1.5 μL of DMSO (3%). Reaction mixtures were incubated in a PCR thermal cycler (Veriti 96-well thermal cycler; Applied Biosystems, Foster City, CA, U.S.A.). Template denaturation and activation of Phusion DNA polymerase for 30 s at 98 °C were followed by 30 cycles of denaturation at 98 °C for 10 s, annealing at 54 °C for 25 s, and extension at 72 °C for 30 s. The reaction was further ended with a final extension step of 10 min at 72 °C and maintained at 4 °C.

Detection of Deafness-Causing Mutations by Using the Silicon-Based SERS Platform. In detail, the prepared AgNPs@Si substrate was first incubated in assembly buffer containing 1 μM hairpin DNA (50 μL, 10 mM phosphate, pH 7.0; Supporting Information Tables S3 and S4) for 24 h. The functionalized platform was subsequently spiked in 0.1 M NaCl phosphate-buffered solution for 14 h to ensure adequate self-assembly between thiolated-DNA and AgNPs@Si. The resultant hairpin DNA-modified AgNPs@Si was then fully purified with 0.1 M PBS solution for several times, and further dried under in air. The surface was subsequently blocked with 1 mM MCH for 10 min to cover the remnant bare region.[19] The PCR products were handled at 95 °C for 30 s to denature the double-stranded DNA, followed by dipping in an ice−water bath for 3 min. After that passivation procedure, the as-treated AgNPs@Si substrate was further hybridized separately with PCR products (the wild type or mutant type) in hybridization buffer (50 μL) for 2.5 h at 37 °C in a sealed centrifuge tube. The samples then underwent a hybridization assay and were prepared for SERS analysis.

RESULTS AND DISCUSSION

A consensus has been reached that AgNPs obtained from various pH values feature different SERS behaviors, which is attributed to distinct size and size distribution of AgNPs.[50,51] While several reports have introduced metal nanoparticles-decorated silicon materials as a kind of SERS substrate, the relationship between morphology of metal nanoparticles (e.g., size and size distribution) and SERS effect remains unknown to date.[22,43,52] Consequently, in this current work, we for the first time investigate distinct SERS performance of the AgNPs@Si induced by different AgNPs morphology in a detailed way. Typically, seven AgNPs@Si samples with different AgNPs morphologies are first prepared via in situ AgNPs growth on the surface of silicon wafers under a series of pH values ranging from 1 to 14 (see experiment details in the Experimental Methods). As shown in Supporting Information Figures S1−S7, morphology of the prepared AgNPs@Si is then systematically characterized using SEM and AFM. Figure 1 presents typical SEM and AFM images of four AgNPs@Si samples prepared at different pH values of 1, 5, 12, and 14 [note that, to guarantee objective comparison, other experiment conditions (e.g., reaction time, temperature, and concentrations of reagents) are all the same in our experiment]. Specifically, in the case of pH values lower than 8 (e.g., 1 and 5), homogeneous nanoparticles with smaller sizes of ∼40−70 nm are produced (Figure 1, parts a−c and e−g). When the pH value gradually increases, AgNPs become larger (∼80−120 nm, pH 12, Figure 1i−k), and eventually aggregated at pH value of 14 (Figure 1m−o). These results clearly indicate that the morphologies (e.g., sizes and distributions) of the AgNPs are distinctly pH-dependent.

To compare the SERS performance of such four kinds of substrates, 10^{-8} M R6G molecules are dispersed on the surface of the prepared AgNPs@Si with a large area (10 μm length ×10 μm width) for SERS mapping test. Parts d, h, l, and p of Figure 1 present typical SERS spectra of R6G recorded from 40 random spots on the substrate, which are obtained under excitation of 633 nm. In particular, AgNPs@Si prepared at pH value of 1 yields feeble Raman signal (∼300; Figure 1d). At pH of 5, the SERS signals increase to ∼2000 (Figure 1h), and reach the highest level (∼18 000) when the pH reaches 12 (Figure 1l), indicating significant AgNPs size-dependent SERS amplification. When pH value further increases to 14, AgNPs of poor monodispersity (some of them are severely aggregated) are observed, producing nonuniform and irreproducible SERS spectra (Figure 1p). These results suggest that the AgNPs@Si prepared at pH value of 12 features the strongest, uniform, and reproducible SERS spectra, which is thus employed for construction of sensors in our following studies.

The prepared seven samples are then utilized for SERS investigation, showing significant AgNPs morphology-dependent SERS performance induced by various pH values. Specifically, the AgNPs@Si yields feeble Raman signals (∼1500) at 1364 cm^{-1} (the C−C stretching mode[53,54]) under acidic conditions (e.g., pH 1, 5). With pH increased to 8, the SERS signals dramatically rise to ∼2500. At pH of 10, the SERS intensities are further enhanced to a higher level (∼10 000), and eventually reach a maximum value (∼18 000) at pH of 12. Afterward, the SERS intensities distinctly decrease to a low value (∼6000) at pH = 13 and further drop to ∼5000 at pH of 14 (Figure 2, parts a and b). The AgNPs@Si at pH of 12 produces the strongest Raman intensity of R6G up to 19 000, remarkably higher than that (<100) of R6G dispersed on pure Si wafer in absence of AgNPs (Figure 2c). On the basis of this, EF values are further calculated by comparing Raman intensities of the AgNPs@Si and pure Si (see details in the Experimental Methods), as presented in Figure 2d. Typically, the three samples prepared at 1, 5, and 8 feature relatively low EF values (<1.0×10^7). With pH value increases, the EF value is increasingly enhanced to ∼2.5×10^7 at pH = 10, and further reaches the maximum value (∼4.5×10^7) at pH of 12. Such distinct EF values of the AgNPs@Si are ascribed to different morphologies of AgNPs distributed on the Si wafer, similar to that of free AgNPs (e.g., previous studies have demonstrated that AgNPs with sizes of ∼80−100 nm produce the strongest SERS signals).[6,10,32,55−58] Typically, the AgNPs@Si samples prepared at pH value ≤10 show relatively poor SERS performance due to smaller sizes (40−70 nm) of AgNPs. With pH value increased to 12, the diameter of AgNPs is correspondingly enhanced to 80−120 nm, yielding an optimum

dx.doi.org/10.1021/ac501675d | Anal. Chem. 2014, 86, 7368−7376

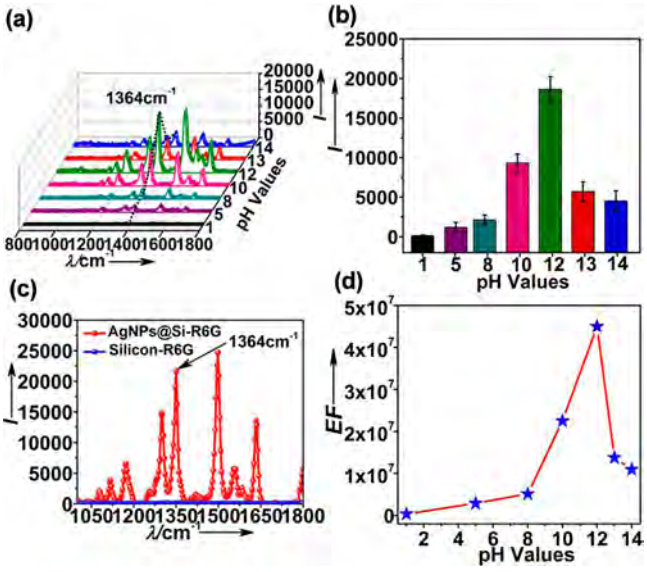

Figure 2. (a) Raman spectrum and (b) corresponding Raman intensities of the 1364 cm^{-1} band of 10^{-8} M R6G dispersed on the surface of AgNPs@Si prepared at varying pHs: black line for pH 1; purple line for pH 5; cyan line for pH 8; pink line for pH 10; olive line for pH 12; red line for pH 13; blue line for pH 14. (c) Raman spectra of R6G (10^{-9} M) immersed on the surface of AgNPs@Si substrate or a pure silicon wafer and (d) enhancement factor (EF) of the AgNPs@Si prepared at different pH values.

EF value of the prepared AgNPs@Si. In addition, AgNPs are effectively coupled and act as high-efficacy hot spots through interconnection to the silicon wafer, which is considered as another significant contributor of the observed giant SERS improvement of the prepared AgNPs@Si.[16,21,32,55] It is worthwhile to point out that appropriate aggregation is favorable for creation of hot spots and enhancement of SERS; nevertheless, severe aggregation is adverse to reproducibility and enhancement of SERS signals (e.g., AgNPs@Si prepared at pH value of 14 produce nonuniform, irreproducible, and poor SERS spectra due to severe aggregation of AgNPs, as shown in Figure 1p), well consistent with previous reports.[22,32,39,52]

In our following studies, the AgNPs@Si with the highest EF value of ~4.5 × 10^7 prepared under optimum conditions (pH 12) are employed for constructing the SERS sensing platform via immobilization of hairpin DNA on its surface. As schematically illustrated in Scheme 1, AgNPs are first in situ grown on the surface of a silicon wafer (1), following by assembly with ROX and thiol molecules-tagged hairpin-structured DNA strands via Ag−S bonds. As a result, significant SERS signals can be detected in such "closed" state since the dyes molecules are near to AgNPs (2; magenta SERS spectra). In the presence of target DNA, SERS intensities are distinctly depressed since adequate hybridization leads to high-efficacy separation between AgNPs and dye molecules (3; black Raman spectra). In comparison, the state keeps "closed" and strong SERS signals are maintained when the noncomplementary DNA is used as a control. Consequently, such signal-off procedure is thus capable of DNA detection based on observing alteration of SERS intensities.

The resultant silicon-based hairpin-assisted SERS platform is superbly suitable for sensitive and specific DNA detection with high reproducibility. As shown in Figure 3a, with concentration

Scheme 1. Schematic Illustration of Silicon-Based Hairpin-Assisted SERS Sensors for DNA Detection[a]

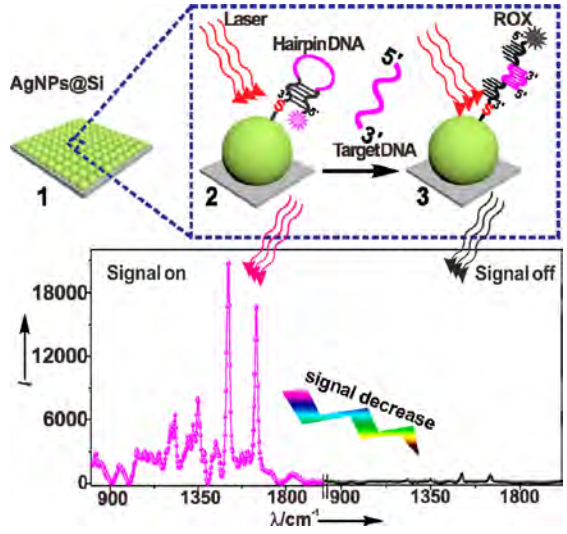

[a]Figure is not to scale.

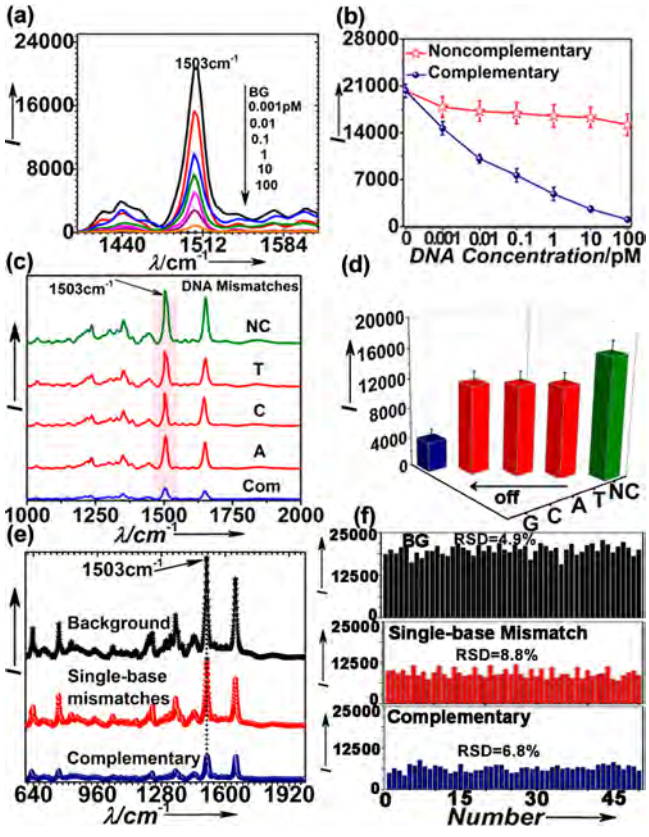

Figure 3. (a) Typical SERS spectra of target DNA at various concentrations ranging from 0.001 to 100 pM. (b) SERS intensity of ROX at 1503 cm^{-1} corresponds to noncomplementary DNA (red) and complementary DNA (blue) of different concentrations. (c) SERS spectra and (d) corresponding Raman intensity (1503 cm^{-1}) of different single-base mismatches. (e) Raman spectra and (f) corresponding Raman intensity (1503 cm^{-1}) recorded from 50 random points in the absence (black) or presence (blue) of complementary DNA, as well as in the presence of single-base mismatches (red).

dx.doi.org/10.1021/ac501675d | Anal. Chem. 2014, 86, 7368−7376

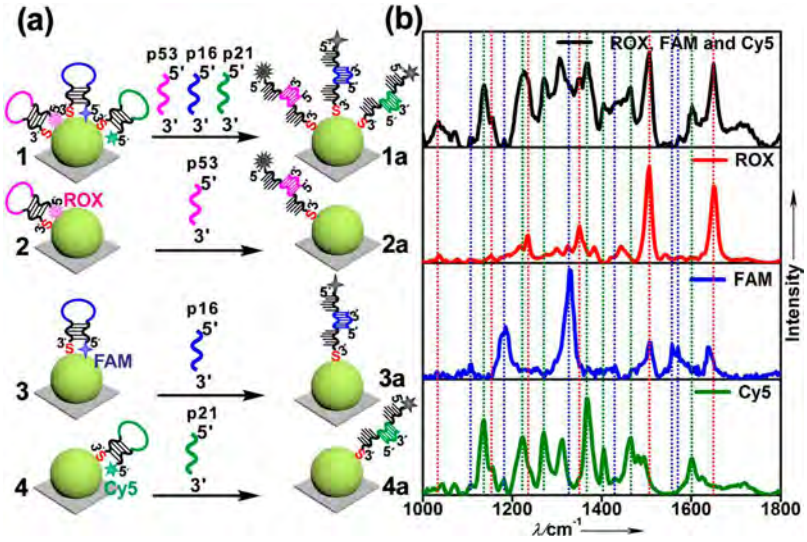

Figure 4. (a) Scheme for the design of the mixed DNA-functionalized AgNPs@Si and (b) corresponding SERS spectrum of the 3-plex probe mixtures used in the multiplexing study (ROX, FAM, Cy5) at a concentration of 1 pM, including individual SERS spectra of each dye-labeled oligonucleotide at a concentration of 1 pM. The three identifying bands from ROX, FAM, and Cy5 are marked on the spectrum (multiplex detection of black line; ROX of red line; FAM of blue line; Cy5 of olive line).

of target DNA gradually decreased from 100 to 0.001 pM, SERS intensities are correspondingly enhanced. Typically, in absence of target DNA (background, BG), one of the representative Raman peaks located at 1503 cm^{-1} exhibits the maximum value of ~19 000 (Figure 3b). Once hybridized with 0.001, 0.01, 0.1, 1, 10, or 100 pM target DNA, the Raman intensity is correspondingly reduced to ~15500, ~11 000, ~7645, ~4860, ~2601, or ~1600, respectively, suggesting a remarkably low detection limit (1 fM). It is worthwhile to point out that previous reports have demonstrated that a few "hot spots" largely contribute to the overall SERS intensity [e.g., there exist just 63 hottest sites ($\eta > 10^9$) in 1 000 000 hot sites, contributing 24% to the overall SERS intensities.[59]]. Consequently, while merely a few hairpins are "opened" by 1 fM target molecules, the signal decrease would be significant in the total signal intensity, well consistent with our experimental data (e.g., ~18% decrease of Raman intensity was observed in the presence of 1 fM target DNA) and previously reported results (e.g., ~30% decrease of Raman intensity was observed in the presence of 0.1 fM complementary target DNA).[60] In addition to ultrahigh sensitivity, the resultant sensor features excellent specificity, allowing facile discrimination of noncomplementary DNA and single-based mismatches. As indicated by a red line in Figure 3b, for the noncomplementary DNA-treated group, the SERS signal preserves a high value of ~16 000−18 000, which is similar to that of the background. When single-base-mismatched targets are employed instead, SERS intensity is reduced to ~12 000, much higher than that of fully complementary DNA (~4500) but lower than that of noncomplementary DNA (~16 500) (Figure 3, parts c and d). Moreover, the prepared sensor possess adaptable reproducibility, producing similar SERS signals adapted from 50 random points with small standard deviation (RSD) values [e.g., 4.9% (background), 8.8% (single-base mismatch), and 6.8% (perfectly complementary target)]. Moreover, small error bars obtained from at least three independent experiments in Figure 3, parts b and d, provide convincing demonstration of the adaptable reproducibility of the as-prepared AgNPs@Si for DNA detection.

Simultaneous detection of multiple analysts in a mixture without separation is of essential importance for molecular detection assays.[1,10,16,32] In our following experiment, multidetection of specific DNA sequences through the selective capture of target strands is performed, which is schematically illustrated in Figure 4a. In brief, three kinds of DNA probes (i.e., ROX-, FAM-, and Cy5-tagged hairpin DNA) are first mixed in the molar ratio of 1:1:1, and then simultaneously assembled with the AgNPs@Si, producing typical SERS signals of the three classes of (1). Different organic dyes (e.g., ROX, FAM, and Cy5) tagged hairpin DNA strands are employed for specifically recognizing corresponding target DNA (2, 3, and 4). In the absence of target DNA, strong background signals are observed. If one certain target DNA (p53, p16, or p21) is added, the action of hybridization to the target sequences would lead to tremendous decrease of the Raman signals via the SERS effect (1a, 2a, 3a, and 4a). In the case of detection of a mixture of three targets DNA, Cy5-, ROX-, and FAM-tagged probes DNA are simultaneously hybridized with their corresponding targets, producing characteristic Raman bands of Cy5, ROX, and FAM, as presented in Figure 4b (black line). Typically, Raman peaks at 1035, 1232, 1350, 1503, and 1649 cm^{-1} belong to the ROX-labeled DNA (Figure 4b, red line); Raman peaks at 1102, 1179, 1322, and 1636 cm^{-1} are ascribed to the FAM-labeled DNA (Figure 4b, blue line); Raman peaks at 1138, 1219, 1267, 1366, 1465, and 1606 cm^{-1} are attributed to the Cy5-labeled DNA (Figure 4b, olive line), indicating that multiple targets DNA could be readily distinguished by using the silicon-based SERS platform.

Deafness is known as the most common sensory deficit in humans.[61] Mutations in more than 60 genes are known to be associated with nonsyndromic hearing loss.[62] To date, there still remains a major challenge to develop facile strategies for rapid and sensitive detection of deafness-causing mutations in a physiological environment, which is of particular significance for early diagnosis and treatment of deafness.[63,64] We thus further employ the silicon-based hairpin DNA-assisted SERS sensor for sensitive discrimination of deafness-causing mutations. To test this idea in a real system, we focus on a deafness

dx.doi.org/10.1021/ac501675d | Anal. Chem. 2014, 86, 7368−7376

gene *SMAC/DIABLO*, single mutation(C377T) in which is identified in an extended Chinese nonsyndromic hearing loss family.[49] In our experiment, to guarantee adequate sensitivity and specificity for detection of the target deafness gene, MCH is first employed to treat the AgNPs@Si substrate.[15,19] On the basis of the DNA sequence of the *SMAC/DIABLO* gene, the perfectly matched and mismatched short DNA fragments (20-mer oligonucleotides) are synthesized as distinct target DNA, and then detected by using the resultant MCH-blocked SERS sensor. Figure 5a displays the Raman spectra of the *SMAC/DIABLO* DNA sequence versus serial concentrations. The Raman intensity is gradually reduced with a concomitant increase in concentration (100 fM to 1 nM). Figure 5b depicts that, with the addition of *SMAC/DIABLO* DNA sequence concentration up to 0.1, 1, 10, 100, or 1000 pM, the corresponding Raman peak intensity drops correspondingly to ~80%, ~68%, ~56%, ~36%, or ~19% of the original intensity. Moreover, the relationship between the concentration of deafness gene and Raman signal well fits the linear correlation (R^2 = 0.994). The prominent 1366 cm^{-1} Raman peak of Cy5 is clearly identifiable at a notably low concentration of 100 fM (i.e., 0.1 pM), indicating the ultrahigh sensitivity of the MCH-blocked SERS sensor. Furthermore, discrimination is best proved by using p1 (single-base-mismatched target) in Figure 5, parts c and d, which induces a 4-fold increased signal in the absence of the perfectly matched target DNA. The p3 (3-bp mismatched target) and p5 (5-bp mismatched target) sequences increases 2.5- and 1.5-fold of signal caused by the perfectly matched target DNA, respectively, demonstrating the excellent SERS selectivity of our method. In addition, small error bars in Figure 5, parts b and d, indicate adaptable reproducibility of the MCH-blocked DNA sensor.

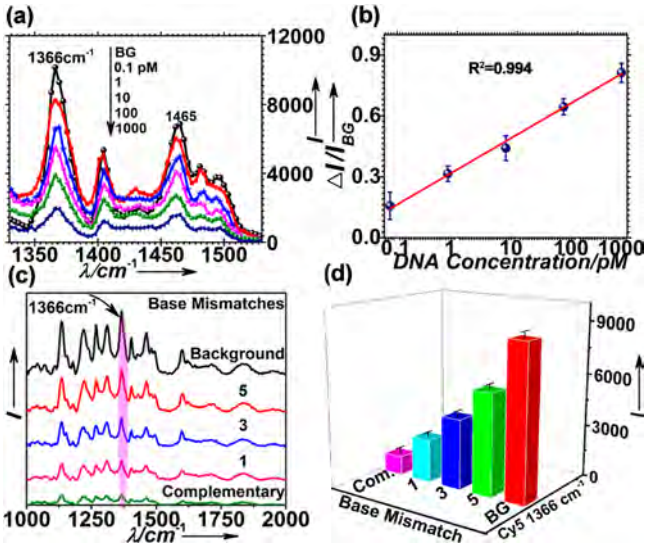

Figure 5. (a) SERS spectra and (b) plot of linear correlation of Raman intensity centered at 1366 cm^{-1} for deafness gene sequence with serial concentrations. (c) Raman spectra and (d) corresponding SERS intensity (1366 cm^{-1}) of different types of single-base-mismatched DNA strands (1 nM). $\Delta I/I_{BG}$ calculated as $(I_{BG} - I_{1366})/I_{BG}$.

Such MCH-blocked silicon-based SERS sensor of high sensitivity and specificity is then employed for the detection of the full-length deafness gene and its mutation in a real system. Figure 6a presents a schematic illustration of the silicon-based SERS sensor for detecting deafness gene sequences. In our experiment, the full-length DNA (720 base pairs) of wild-type *SMAC/DIABLO* or mutant form (*SMAC/DIABLO*^{C377T}) is amplified by PCR and then followed by DNA extraction and DNA sequencing analysis, demonstrating accurate sequences of the resultant PCR products.[49] These PCR products [the wild type (WT) or mutant type (MT)] are further handled at 95 °C for 30 s to denature the double-stranded DNA, followed by dipping in an ice−water bath for 3 min (step 1), which is finally utilized for deafness detection by

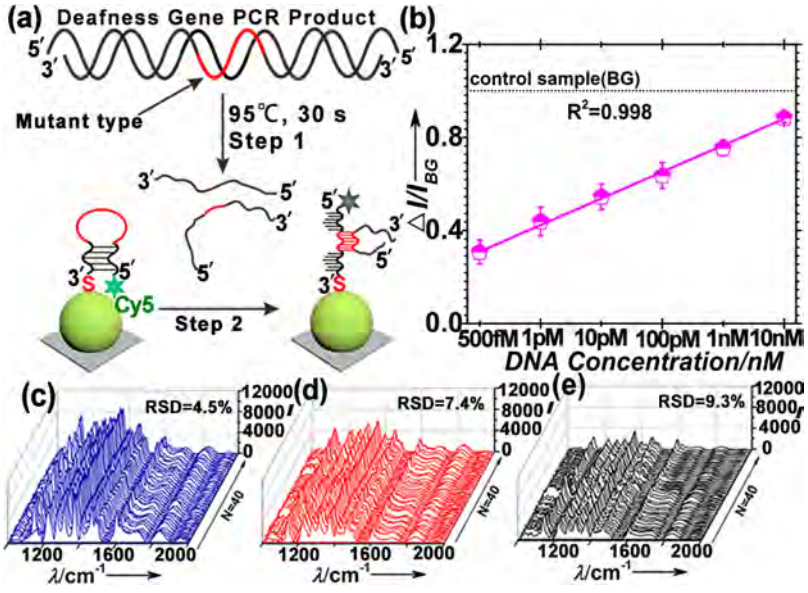

Figure 6. (a) Schematic diagram of silicon-based SERS sensor for deafness gene detection and (b) the linear relationship of Raman intensity of 1366 cm^{-1} band as a function of the wild-type concentrations from 500 fM to 10 nM. $\Delta I/I_{BG}$ calculated as $(I_{BG} - I_{1366})/I_{BG}$. (c) Raman mapping spectra of Cy5 in the absence of wild/mutant gene (background). (d) Raman mapping spectra of Cy5 in the presence of the mutant type (red line) or (e) the wild type (black line).

dx.doi.org/10.1021/ac501675d | *Anal. Chem.* 2014, 86, 7368−7376

using the MCH-blocked SERS sensor (step 2, see experiment details in the Experimental Methods). Figure 6b depicts a good linear relationship between $\Delta I/I_{BG}$ values and concentrations of the WT ranging from 500 fM to 10 nM (R^2 = 0.998, please see the corresponding SERS spectra in Supporting Information Figure S8), suggesting a remarkably low DNA detection limit (500 fM) in a real system, much lower than that (5 nM) ever reported by conventional methods [e.g., allele-specific PCR, DNA sequencing, PCR-RFLP analysis, and allele-specific oligonucleotide hybridization (ASO)[65]]. A single-base mismatch introduced by changing C to T in the target sequence is further employed to test the detection specificity. Typically, as shown in Figure 6c–e, the intensity of the MT (~6000) is distinctively larger than that of the WT (~3500), which is due to good specificity of the resultant sensor. In addition to the high sensitivity and specificity, our sensor for deafness detection is highly reproducible, producing uniform Raman spectra obtained from 40 random points on the AgNPs@Si substrates with small RSD values [4.5% (background), 7.4% (MT), and 9.3% (WT), respectively].

CONCLUSIONS

To be summarized, we present a kind of high-performance SERS sensing platform made of hairpin DNA-modified AgNPs@Si, which can be facilely and rapidly prepared via a one-step in situ growth of AgNPs on silicon wafer. On the basis of systematical investigation of the relationship between SERS effect and morphology of AgNPs, optimum reaction conditions (i.e., pH = 12, reaction time = 20 min) are achieved to produce the AgNPs@Si with a high EF of ~10^7 and excellent reproducibility. Such high-quality AgNPs@Si is then employed for construction of a silicon-based SERS sensing platform through self-assembly of hairpin DNA. As a proof-in-principle experiment, a detection limit of 1 fM is readily obtained in a very reproducible manner along with high specificity. Most significantly, for the first time, the silicon-based SERS sensor is further employed as a practical tool for deafness-causing mutation detection, with a remarkably low detection limit (500 fM) in a real system, much better than that (~5 nM) ever reported by conventional strategies. Given that the silicon-based SERS substrates can be facilely and rapidly prepared at low cost, we expect this hairpin DNA-assisted "signal-off" SERS platform may open up exciting avenues toward practical SERS applications for disease diagnosis, food safety, drug security, as well as environment monitoring and so forth.

ASSOCIATED CONTENT

Supporting Information

SEM, AFM, and Raman spectra of AgNPs@Si. This material is available free of charge via the Internet at http://pubs.acs.org.

AUTHOR INFORMATION

Corresponding Authors

*E-mail: hesudan@suda.edu.cn. Fax: +86-512-65880899-3623.
*E-mail: yaohe@suda.edu.cn. Fax: +86-512-65880946.

Author Contributions

§H.W., X.X.J., and X.W. contributed equally to this work.

Notes

The authors declare no competing financial interest.

ACKNOWLEDGMENTS

We thank Dr. Huijun Yuan (Chinese PLA General Hospital) for providing mutant *SMAC/DIABLO* plasmid DNA. The authors appreciate financial support from the National Basic Research Program of China (973 Program 2013CB934400 and 2013CB910102), the Funds for International Cooperation and Exchange of the National Natural Science Foundation of China (Grant No. 61361160412), NSFC (Grants 30900338, 51072126, and 51132006), the Natural Science Foundation of Jiangsu Province of China (Grant Nos. BK20130052 and BK20130298), the Specialized Research Fund for the Doctoral Program of Higher Education of China (Grant Nos. 20133201110019 and 20133201120024), and a project funded by the Priority Academic Program Development of Jiangsu Higher Education Institutions (PAPD).

REFERENCES

(1) Nie, S. M.; Emory, S. R. *Science* **1997**, *275*, 1102–1106.
(2) Cao, Y. W. C.; Jin, R. C.; Mirkin, C. A. *Science* **2002**, *297*, 1536–1540.
(3) Tognalli, N. G.; Cortés, E.; Hernández-Nieves, A. D.; Carro, P.; Usaj, G.; Balseiro, C. A.; Vela, M. E.; Salvarezza, R. C.; Fainstein, A. *ACS Nano* **2011**, *5*, 5433–5443.
(4) Kim, N. H.; Lee, S. J.; Moskovits, M. *Nano Lett.* **2010**, *10*, 4181–4185.
(5) Chen, G.; Wang, Y.; Yang, M. X.; Xu, J.; Goh, S. J.; Pan, M.; Chen, H. Y. *J. Am. Chem. Soc.* **2010**, *132*, 3644–3645.
(6) Ochsenkühn, M. A.; Jess, P. R. T.; Stoquert, H.; Dholakia, K.; Campbell, C. J. *ACS Nano* **2009**, *3*, 3613–3621.
(7) Shafer-Peltier, K. E.; Haynes, C. L.; Glucksberg, M. R.; Van Duyne, R. P. *J. Am. Chem. Soc.* **2003**, *125*, 588–593.
(8) Dasary, S. S. R.; Singh, A. K.; Senapati, D.; Yu, H. T.; Ray, P. C. *J. Am. Chem. Soc.* **2009**, *131*, 13806–13812.
(9) Qian, X. M.; Zhou, X.; Nie, S. M. *J. Am. Chem. Soc.* **2008**, *130*, 14934–14935.
(10) Kang, T.; Yoo, S. M.; Yoon, I.; Lee, S. Y.; Kim, B. *Nano Lett.* **2010**, *10*, 1189–1193.
(11) Cao, Y. C.; Jin, R. C.; Nam, J. M.; Thaxton, C. S.; Mirkin, C. A. *J. Am. Chem. Soc.* **2003**, *125*, 14676–14677.
(12) Bonham, A. J.; Braun, G.; Pavel, I.; Moskovits, M.; Reich, N. O. *J. Am. Chem. Soc.* **2007**, *129*, 14572–14573.
(13) Du, J.; Liu, M. Y.; Lou, H. X.; Zhao, T.; Wang, Z.; Xue, Y.; Zhao, J. L.; Xu, Y. S. *Anal. Chem.* **2012**, *84*, 8060–8066.
(14) Lee, S. J.; Moskovits, M. *Nano Lett.* **2011**, *11*, 145–150.
(15) Braun, G.; Lee, S. J.; Dante, M.; Nguyen, T. Q.; Moskovits, M.; Reich, N. *J. Am. Chem. Soc.* **2007**, *129*, 6378–6379.
(16) He, Y.; Su, S.; Xu, T. T.; Zhong, Y. L.; Zapien, J. A.; Li, J.; Fan, C. H.; Lee, S. T. *Nano Today* **2011**, *6*, 122–130.
(17) Miranda-Castro, R.; de-los-Santos-Álvarez, P.; Lobo-Castañón, M. J.; Miranda-Ordieres, A. J.; Tuñón-Blanco, P. *Anal. Chem.* **2007**, *79*, 4050–4055.
(18) Liu, G.; Wan, Y.; Gau, V.; Zhang, J.; Wang, L. H.; Song, S. H.; Fan, C. H. *J. Am. Chem. Soc.* **2008**, *130*, 6820–6825.
(19) Fan, C. H.; Plaxco, K. W.; Heeger, A. J. *Proc. Natl. Acad. Sci. U.S.A* **2003**, *100*, 9134–9137.
(20) Du, H.; Strohsahl, C. M.; Camera, J.; Miller, B. L.; Krauss, T. D. *J. Am. Chem. Soc.* **2005**, *127*, 7932–7940.
(21) Su, S.; Wei, X. P.; Zhong, Y. L.; Guo, Y. Y.; Su, Y. Y.; Huang, Q.; Lee, S. T.; Fan, C. H.; He, Y. *ACS Nano* **2012**, *6*, 2582–2590.
(22) Wei, X. P.; Su, S.; Guo, Y. Y.; Jiang, X. X.; Zhong, Y. L.; Su, Y. Y.; Fan, C. H.; Lee, S. T.; He, Y. *Small* **2013**, *9*, 2493–2499.
(23) He, Y.; Zhong, Y. L.; Peng, F.; Wei, X. P.; Su, Y. Y.; Lu, Y. M.; Su, S.; Gu, W.; Liao, L. S.; Lee, S. T. *J. Am. Chem. Soc.* **2011**, *133*, 14192–14195.
(24) He, Y.; Zhong, Y. L.; Peng, F.; Wei, X. P.; Su, Y. Y.; Su, S.; Gu, W.; Liao, L. S.; Lee, S. T. *Angew. Chem., Int. Ed.* **2011**, *50*, 3080–3083.

(25) Zhong, Y. L.; Peng, F.; Wei, X. P.; Zhou, Y. F.; Wang, J.; Jiang, X. X.; Su, Y. Y.; Su, S.; Lee, S. T.; He, Y. *Angew. Chem., Int. Ed.* **2012**, *51*, 8485−8489.
(26) Peng, F.; Su, Y. Y.; Wei, X. P.; Lu, Y. M.; Zhou, Y. F.; Zhong, Y. L.; Lee, S. T.; He, Y. *Angew. Chem., Int. Ed.* **2013**, *52*, 1457−1461.
(27) He, Y.; Zhong, Y. L.; Su, Y. Y.; Lu, Y. M.; Jiang, Z. Y.; Peng, F.; Xu, T. T.; Su, S.; Huang, Q.; Fan, C. H.; Lee, S. T. *Angew. Chem., Int. Ed.* **2011**, *50*, 5695−5698.
(28) Zhong, Y. L.; Peng, F.; Bao, F.; Wang, S. Y.; Ji, X. Y.; Yang, L.; Su, Y. Y.; Lee, S. T.; He, Y. *J. Am. Chem. Soc.* **2013**, *135*, 8350−8356.
(29) Sharon, E.; Freeman, R.; Riskin, M.; Gil, N.; Tzfati, Y.; Willner, I. *Anal. Chem.* **2010**, *82*, 8390−8397.
(30) Shimron, S.; Cecconello, A.; Lu, C. H.; Willner, I. *Nano Lett.* **2013**, *13*, 3791−3795.
(31) Freeman, R.; Willner, I. *Chem. Soc. Rev.* **2012**, *41*, 4067−4085.
(32) He, Y.; Fan, C. H.; Lee, S. T. *Nano Today* **2010**, *5*, 282−295.
(33) Graham, D.; Thompson, D. G.; Smith, W. E.; Faulds, K. *Nat. Nanotechnol.* **2008**, *3*, 548−551.
(34) Lim, D. K.; Jeon, K. S.; Hwang, J. H.; Kim, H.; Kwon, S.; Suh, Y. D.; Nam, J. M. *Nat. Nanotechnol.* **2011**, *6*, 452−460.
(35) Scrimshaw, B. J.; Faed, J. M.; Tate, W. P.; Yun, K. *J. Hum. Genet.* **1999**, *44*, 388−390.
(36) Li, Z.; Li, R.; Chen, J.; Liao, Z.; Zhu, Y.; Qian, Y.; Xiong, S.; Heman-Ackah, S.; Wu, J.; Choo, D. I.; Guan, M. X. *Hum. Genet.* **2005**, *117*, 9−15.
(37) Berrettini, S.; Forli, F.; Passetti, S.; Rocchi, A.; Pollina, L.; Cecchetti, D.; Mancuso, M.; Siciliano, G. *Biosci. Rep.* **2008**, *28*, 49−59.
(38) Su, Y. Y.; Wei, X. P.; Peng, F.; Zhong, Y. L.; Lu, Y. M.; Su, S.; Xu, T. T.; Lee, S. T.; He, Y. *Nano Lett.* **2012**, *12*, 1845−1850.
(39) Jiang, X. X.; Jiang, Z. Y.; Xu, T. T.; Su, S.; Zhong, Y. L.; Peng, F.; Su, Y. Y.; He, Y. *Anal. Chem.* **2013**, *85*, 2809−2816.
(40) Huang, Z. L.; Meng, G. W.; Huang, Q.; Yang, Y. J.; Zhu, C. H.; Tang, C. L. *Adv. Mater.* **2010**, *22*, 4136−4139.
(41) Xu, T. T.; Huang, J. A.; He, L. F.; He, Y.; Su, S.; Lee, S. T. *Appl. Phys. Lett.* **2011**, *99*, 153116.
(42) He, L. F.; Huang, J. A.; Xu, T. T.; Chen, L. M.; Zhang, K.; Han, S. T.; He, Y.; Lee, S. T. *J. Mater. Chem.* **2012**, *22*, 1370−1374.
(43) Li, W. Y.; Camargo, P. H. C.; Lu, X. M.; Xia, Y. N. *Nano Lett.* **2009**, *9*, 485−490.
(44) Payne, E. K.; Rosi, N. L.; Xue, C.; Mirkin, C. A. *Angew. Chem., Int. Ed.* **2005**, *44*, 5064−5067.
(45) Qian, X. M.; Nie, S. M. *Chem. Soc. Rev.* **2008**, *37*, 912−920.
(46) Song, S. P.; Liang, Z. Q.; Zhang, J.; Wang, L. H.; Li, G. X.; Fan, C. H. *Angew. Chem., Int. Ed.* **2009**, *48*, 8670−8674.
(47) Zhang, Y. G.; Lu, F.; Yager, K. G.; van der Lelie, D.; Gang, O. *Nat. Nanotechnol.* **2013**, *8*, 865−872.
(48) Dodge, A.; Turcatti, G.; Lawrence, I.; de Rooij, N. F.; Verpoorte, E. *Anal. Chem.* **2004**, *76*, 1778−1787.
(49) Cheng, J.; Zhu, Y. H.; He, S. D.; Lu, Y. P.; Chen, J.; Han, B.; Petrillo, M.; Wrzeszczynski, K. O.; Yang, S. M.; Dai, P.; Zhai, S. Q.; Han, D. Y.; Zhang, M. Q.; Li, W.; Liu, X. Z.; Li, H. W.; Chen, Z. Y.; Yuan, H. J. *Am. J. Hum. Genet.* **2011**, *89*, 56−66.
(50) Singh, M.; Sinha, I.; Mandal, R. K. *Mater. Lett.* **2009**, *63*, 425−427.
(51) Chen, Y.; Wang, C. G.; Ma, Z. F.; Su, Z. M. *Nanotechnology* **2007**, *18*, 325602.
(52) Jiang, Z. Y.; Jiang, X. X.; Su, S.; Wei, X. P.; Lee, S. T.; He, Y. *Appl. Phys. Lett.* **2012**, *100*, 203104.
(53) Michaels, A. M.; Nirmal, M.; Brus, L. E. *J. Am. Chem. Soc.* **1999**, *121*, 9932−9939.
(54) Rycenga, M.; Xia, X. H.; Moran, C. H.; Zhou, F.; Qin, D.; Li, Z. Y.; Xia, Y. N. *Angew. Chem., Int. Ed.* **2011**, *50*, 5473−5477.
(55) Peng, Z. P.; Hu, H. L.; Utama, M. I. B.; Wong, L. M.; Ghosh, K.; Chen, R. J.; Wang, S. J.; Shen, Z. X.; Xiong, Q. H. *Nano Lett.* **2010**, *10*, 3940−3947.
(56) Chen, R. J.; Li, D. H.; Hu, H. L.; Zhao, Y. Y.; Wang, Y.; Wong, N.; Wang, S. J.; Zhang, Y.; Hu, J.; Shen, Z. X.; Xiong, Q. H. *J. Phys. Chem. C* **2012**, *116*, 4416−4422.
(57) Fang, C.; Agarwal, A.; Widjaja, E.; Garland, M. V.; Wong, S. M.; Linn, L.; Khalid, N. M.; Salim, S. M.; Balasubramanian, N. *Chem. Mater.* **2009**, *21*, 3542−3548.
(58) Zhang, J.; Song, S. P.; Wang, L. H.; Pan, D.; Fan, C. H. *Nat. Protoc.* **2007**, *2*, 2888−2895.
(59) Fang, Y.; Seong, N. H.; Dlott, D. D. *Science* **2008**, *321*, 388−392.
(60) Ngo, H. T.; Wang, H. N.; Fales, A. M.; Vo-Dinh, T. *Anal. Chem.* **2013**, *85*, 6378−6383.
(61) Morton, C. C.; Nance, W. E. *N. Engl. J. Med.* **2006**, *354*, 2151−2164.
(62) Shearer, A. E.; Smith, R. J. H. *Curr. Opin. Pediatr.* **2012**, *24*, 679−686.
(63) Schrauwen, I.; Sommen, M.; Corneveaux, J. J.; Reiman, R. A.; Hackett, N. J.; Claes, C.; Claes, K.; Bitner-Glindzicz, M.; Coucke, P.; Camp, G. V.; Huentelman, M. J. *Am. J. Med. Genet., Part A* **2013**, *161*, 145−152.
(64) Mamanova, L.; Coffey, A. J.; Scott, C. E.; Kozarewa, I.; Turner, E. H.; Kumar, A.; Howard, E.; Shendure, J.; Turner, D. J. *Nat. Methods* **2010**, *7*, 111−118.
(65) Tang, H. Y.; Hutcheson, E.; Neill, S.; Drummond-Borg, M.; Speer, M.; Alford, R. L. *Genet. Med.* **2002**, *4*, 336−345.

中文摘要

Wang H, Jiang X, Wang X, Wei X, Zhu Y, Sun B, Su Y, He S*, He Y*. A hairpin DNA-assisted silicon/silver based surface enhanced raman scattering platform for ultrahighly sensitive and specific discrimination of deafness mutations in a real system. Anal Chem；2014 Aug 5;86:7368-76. (*共同通讯作者)（IF= 5.636，他引次数：4）

表面增强拉曼散射（SERS）是公认的功能强大的分析工具，用于超高灵敏度的检测分析物。在这篇文章中，我们提出了一种硅基 SERS 检测平台，由一个发夹 DNA 修饰的银纳米颗粒修饰硅片(AgNPs@Si)。尤其是，我们系统研究发现 AgNPs@Si 在最佳反应条件下（即 PH 值= 12，反应时间 = 20 分钟)首次实现增强因子（EF）为~4.5×10^7。这样合成的 AgNPs@Si 然后构建一个硅基 SERS 检测平台，通过表明修饰发夹 DNA，这个非常适合于高重复性、多元性以及超灵敏性的 DNA 检测。1fM 的检出限可以得到实现，而且具有可重复和高特异性。最重要的是，我们首次证明了硅基 SERS 平台可以在一个 femtomolar 水平（500 fM）的实际系统中高效鉴别耳聋的致病突变体，大约是 3−4 数量低于常规检测水平（~5 nm）。我们的研究结果提供了 SERS 应用于生物医学的尝试，并展现了令人兴趣的潜能。